GeoScienceWorld
Lithosphere
Volume 2023, Article ID lithosphere_2023_166, 17 pages
https://doi.org/10.2113/2023/lithosphere_2023_166

Lithosphere

Research Article

The Late Paleocene–Eocene Extension and Differential Denudation in the Eastern Daqingshan Mountains Around the Northeastern Margin of the Ordos Block, Western North China Craton, Constrained by Apatite (U-Th)/He Thermochronology

Lixia Feng,[1] **Baofu Han**,[2] **Lin Wu**,[3] **Zhongpeng Han**,[4] **Jiawei Zhang**,[5] **and Mei Liu**[1]

[1]*School of Emergency Science, Xihua University, Chengdu 610039, China*
[2]*Key Laboratory of Orogenic Belts and Crustal Evolution, Ministry of Education/School of Earth and Space Sciences, Peking University, Beijing 100871, China*
[3]*State Key Laboratory of Lithospheric Evolution, Institution of Geology and Geophysics, Chinese Academy of Sciences, Beijing 100029, China*
[4]*Institute of Earth Sciences, China University of Geosciences, Beijing 100083, China*
[5]*Institute of Geology, China Earthquake Administration, Beijing 100029, China*

Correspondence should be addressed to Lin Wu; wulin08@mail.iggcas.ac.cn

Received 12 April 2023; Accepted 17 August 2023; Published 11 September 2023

Academic Editor: Xiaoming Shen

The initial timing of extension during the Cenozoic around the northeastern margin of the Ordos Block, western North China Craton (NCC), is still poorly constrained. Apatite (U-Th)/He low-temperature thermochronology was thus applied on eight pre-Cenozoic granitic and gneissic samples transecting the eastern Daqingshan Mountains, northeastern margin of the Ordos Block, to investigate the denudation and cooling event related to the onset of extension therein. Four mean corrected AHe ages in the southern part are overlapped within the standard deviations of 50.0 ± 0.4 to 45.0 ± 8.0 Ma. However, three mean corrected AHe ages in the northern part are prominently older of 99.2 ± 11.0 to 86.6 ± 17.1 Ma, with the rest one of 56.1 ± 8.6 Ma. Altogether, they show a younger-older-younger-older pattern along the transect correlated with the normal faults. AHe thermal history modeling results further demonstrate extensive cooling during the Late Cretaceous but differential cooling during the Late Paleocene–Eocene. The Late Cretaceous extensive cooling in the eastern Daqingshan Mountains, as well as the contemporaneous deposition hiatus in both the eastern Daqingshan Mountains and the Hohhot Depression, together indicates overall denudation in the northeastern margin of the Ordos Block at that time. The Late Paleocene–Eocene differential cooling is probably induced by the tilting of the eastern Daqingshan Mountains as a result of the extension suggested by the distribution of AHe ages. It corresponds to the syn-tectonic subsidence in the Hohhot Depression, indicating a basin-mountain coupling. Regional comparative analysis manifests similar extension around the Ordos Block and more widely across the NCC during the Late Paleocene–Eocene. Temporally, kinematically, and dynamically coupled with this regional extension event, the subduction of the Izanagi-Pacific plate probably plays a major role. However, the contribution of the India-Asia collision could not be ignored.

1. Introduction

During the Cenozoic, much of East Asia experienced intense intraplate deformation [1, 2], influenced by the subduction of the Izanagi-Pacific plate under the Eurasian plate to the east [3–5] or the collision of the Indo-Eurasian plate to the southwest [6–9] or their combined effect. Notably in the western North China Craton (NCC), the

hinterland of East Asia, a multistage of intraplate deformation developed in the periphery of the Ordos Block (Figure 1), forming the special "Ring-shaped" rift systems [10–16]. In order to explore the geodynamics of the rift systems with such a pattern, numerous geo/thermochronological studies, structure kinematic and geometric studies, basin analysis, and fieldwork have been carried out in the rift basins and the adjoining mountains (Figure 1), such as the Shanxi Rift System around the eastern and southeastern margin [17–20], the Yinchuan Basin and the Helanshan Mountains around the western margin [21–23], the Hetao Basin [24–26], the Langshan and Seertengshan Mountains around the northwestern margin [27–29], the Wulashan and western Daqingshan Mountains [30–32] around the northern margin, and the eastern Daqingshan Mountains around the northeastern margin [33–35]. The results of these researches provide important geological evidence linking the intraplate deformation therein with the subduction and collision of the abovementioned plates. However, the timing of incipient extension in the northeastern margin of the Ordos Block is still controversial: one school of opinion proposed that extension was initiated since the Miocene [16], while the others held that extension had already started during the Eocene [36]. Obviously, this divergence restricts the overall understanding of the geodynamics of the rift systems around the Ordos Block and even the intraplate deformation in the broader region during the Cenozoic.

The northeastern margin of the Ordos Block is composed of the eastern Daqingshan Mountains and the easternmost part of the Hetao Basin (Hohhot Depression; Figure 1). The disagreement on the onset of extension mainly originates from the division of the Tertiary syntectonic stratigraphic sequence in the Hohhot Depression based on drilling and seismic data [24, 25, 33, 36]. As for the eastern Daqingshan Mountains, although the apatite fission track (AFT) thermochronology therein displayed Cenozoic cooling signature before Miocene [35], the causal relationship between the Cenozoic cooling event and extension was not directly correlated. However, the revealed Cenozoic cooling range corresponds well to the partial retention zone (PRZ) of the apatite (U-Th)/He (AHe) dating system. Therefore, this paper carried out AHe thermochronology on the footwall rocks traversing the eastern Daqingshan Mountains (Figure 2) in order to constrain the timing of the Cenozoic initial cooling event and its relationship with extension. It will provide new thermochronological evidence to the study of the geodynamics of the northeastern part of the rift systems around the Ordos Block.

2. Geological Setting

The eastern Daqingshan Mountains and the Hohhot Depression constitute the northeastern margin around the Ordos Block (Figure 1). Topographically, the eastern Daqingshan Mountains, with the main peak at 2338 m above sea level (asl), descend SE rapidly to the Hohhot Depression at ca. 1000 m asl. They are separated by the normal fault F_1 (Figure 2). It is widely accepted that the normal fault F_1 controlled the differential uplift-denudation of the eastern Daqingshan Mountains and subsidence-sedimentation of the Hohhot Depression during the Cenozoic, forming the current basin-mountain morphotectonic pattern [30, 34, 36]. Whereas to the NW, the eastern Daqingshan Mountains decrease gently to the Mongolian Plateau at ca. 1500 m asl. They are separated by the normal fault F_2 (Figure 2).

The eastern Daqingshan Mountains mainly consist of Precambrian metamorphic rocks and Upper Jurassic–Lower Cretaceous, with sporadic spread of Paleozoic and Cenozoic sedimentary rocks (Figure 2; [37–39]). Specifically, the Cenozoic strata contain the Pliocene clastic rocks with calcareous nodules and gypsum interlayers and the Quaternary alluvial deposits, slope deposits, and loess [37]. Besides, the Early Proterozoic to Early Cretaceous granitoids are also distributed in the study area [40–42].

The eastern Daqingshan Mountains underwent complex extensional and compressional deformations in the Late Mesozoic [41, 43–49], including the Panyangshan thrusts (PST), Hohhot metamorphic core complex (MCC), and Daqingshan thrust-nappe system (DSTS). The north-tilting PST is located in the northeastern part of the eastern Daqingshan Mountains to the north of Wulanheya (Figure 2). It was active during the Late Jurassic to Early Cretaceous [48, 50] and carried the Archaean gneisses atop the Late Proterozoic marbles, both of which overrode the Carboniferous gray-black conglomerates (Figure 2). The Hohhot MCC is located in the central part of the eastern Daqingshan Mountains and contains three near EW-striking detachment faults (Figure 2; [48]). Zircon U-Pb ages of the syn-tectonic mylonitic granite and the undeformed granite in the ductile shear zones constrain the timing of the ductile shearing of the Hohhot MCC at deep levels between 142 and 132 Ma [41]. The DSTS contains three major southeast-tilting thrusts (Figure 2; [48]). $^{40}Ar/^{39}Ar$ ages of the syn-tectonic mica indicate the DSTS was active at ca. 120 Ma during its late stage [46]. However, hornblende, mica, biotite, and k-feldspar $^{40}Ar/^{39}Ar$ ages also indicate rapid denudation and cooling of the ductile shear zone about the same time [45, 47–49]. Anyway, this period of rapid denudation and cooling is considered to correlate with the activities of either the detachment faults of the Hohhot MCC [45, 47, 49] or the DSTS [46, 48].

The Hohhot Depression to the southeast of the eastern Daqingshan Mountains is the easternmost part of the Hetao Basin (Figure 1). The Hetao Basin is a Meso-Cenozoic rift basin located between the Ordos Block and the Langshan, Seertengshan, and Daqing Mountains with a convex generally toward the northwest (Figure 1). It includes five secondary units, namely Linhe Depression (or Jilantai Basin), Wulashan Mountain Uplift, Wuqian Depression, Baotou Uplift, and Hohhot Depression from west to east [26]. Borehole and geophysical studies through lithofacies and fossil analysis have been carried out in the Hohhot Depression [24, 25, 33, 36, 51]. Seismic interpretation results indicate that the Cenozoic sedimentary rocks near Hohhot are syn-tectonic with the normal fault F_1

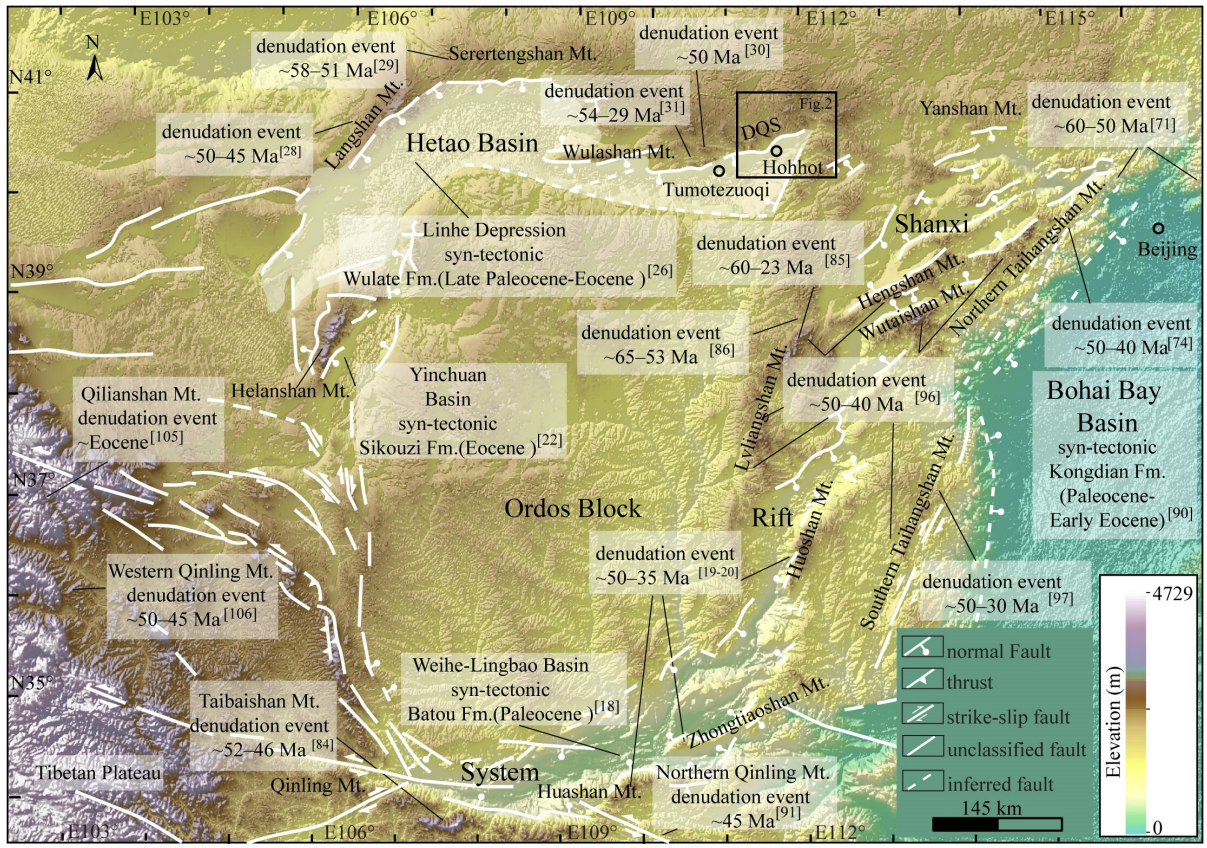

Figure 1: DEM map of the Ordos block with simplified structures and indications of the Paleocene-Eocene denudation events demonstrated by thermochronological studies and contemporaneous strata nearby. Simplified structures are modified after References 16, 19. Abbreviations: Mt, Mountains; DQS, the Daqingshan Mountains.

[25], and the thickness exceeds 7000 m [36]. However, the division of the Tertiary strata in the Hohhot depression is debatable (Figure 2(b); from bottom to top): the Wuyuan and Wulantuke Fm [24] or the Wulate, Linhe, Wuyuan, and Wulantuke Fm [33]. Drilling data from He-1 near Tumotezuoqi (Figure 1) indicate the Wuyuan Fm. to the Miocene [24], whereas ostracoda, stonewort, and sporopollen fossil from Drilling Bitan-1 near Hohhot (Figure 1) indicate the age of the Wulate Fm. to the Late Paleocene–Early Eocene [33]. Either way, the bottom Tertiary strata mainly of conglomerate rocks unconformably overlie the Lower Cretaceous.

The dividing normal faults F_1 and F_2 (Figure 2) are both active during the Cenozoic [52, 53]. However, strata data show the extension of the normal fault F_1 between the eastern Daqingshan Mountains and the Hohhot depression is much more intense [36]. It strikes north-east-east (NEE) with dip of ca. ∠50° measured from the outcropped fault cliffs, on which three sets of striations are recognized: nearly NW-SE extension in the early stage, NE-SW extension in the middle stage, and almost N-S extension in the late stage [16], suggesting multistage of extension. The deep seismic reflection profile shows that the normal fault F_1 is formed by the downward merging of three high-angle normal faults dipping to the south with a spade-shape in the deep and cutting the Cretaceous, Tertiary, and Quaternary in the Hohhot depression [25]. Importantly, the contact of these normal faults with the Cenozoic strata shows syn-sedimentary [25], indicating that the activity of the normal fault F_1 is multistage as well. However, mainly owing to the divergence about the basal Tertiary strata, the timing of the initial extension is accordingly in dispute: the Eocene [36] or Miocene [16]. Paleo-earthquake data further indicate that it is still active currently [52]. In addition, the normal fault F_2 between the eastern Daqingshan Mountains and the Mongolian Plateau (Figure 2) has a long-term activity history since the Mesoproterozoic [53]. It is probably reactivated during the Cenozoic as an accommodation of the normal fault F_1 [53].

3. Sampling and Method

Eight samples were collected along the NW-SE orientated Kuisu-Dalanqi profile across the eastern Daqingshan Mountains (Figure 2). Sample D18-11 is the Early Cretaceous mylonitic granite collected in the ductile shear zone of the Hohhot MCC with obvious foliation and lineation (Figure 3(a)). Samples D18-16 and D18-17 are granitic gneiss dated back to Paleoproterozoic (Figures 3(d)–3(e)). The other samples, D18-12 to D18-14 (Figures 3(b)–3(c)) and D18-22 to D18-24 (Figures 3(f)–3(i)) are granite emplaced during the Early Cretaceous and Permian,

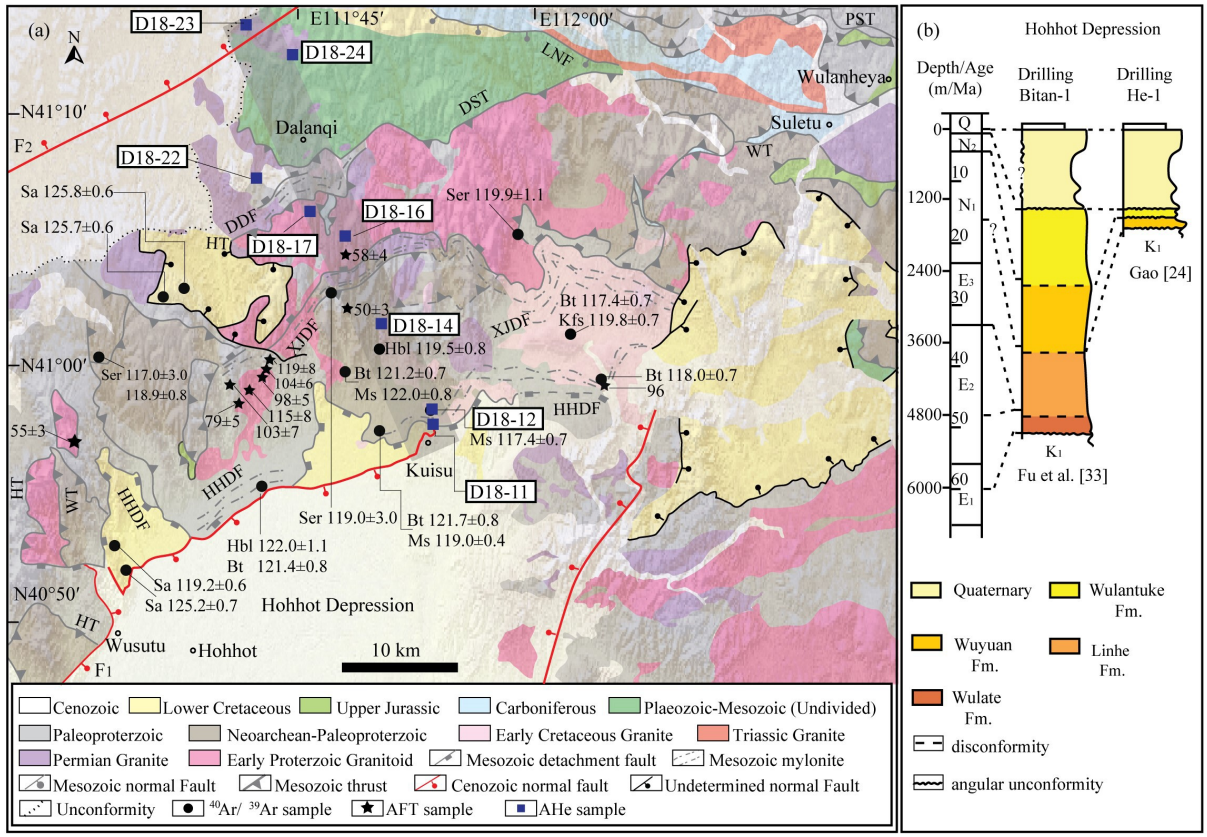

FIGURE 2: (a) Geological and structural map of the eastern Daqingshan Mountains overlapped on the DEM map, Mesozoic structures are modified after Reference 48, Cenozoic structures are modified after References 36, 37, $^{40}Ar/^{39}Ar$ data are from References 14, 47, 48, AFT data are from References 34, 35, 47, Age unit: Ma; (b) Cenozoic stratal sequences of the Hohhot Depression based on two different division schemes, the thickness value of Quaternary is not given in Reference 33 and that from Reference 24 is referred in the middle column. Abbreviations: PST, the Panyangshan thrusts; DST, the Daqingshan thrust; HT, the Huangtuyaozi-Majiadian-Deshengying thrust; WT, the Wusutu-Huanghuawopu-Suletu thrust; DDF, the Deshengying detachment fault; XJDF, the Xiaojing detachment fault; HHDF, the Hohhot detachment fault; Hbl, hornblende; Ser, sericite; Ms, muscovite; Bt, biotite; Kfs, k-Feldspar; Sa, sanidine; E_1, Paleocene; E_2, Eocene; E_3, Oligocene; N_1, Miocene; N_2, Pliocene.

respectively. Their elevations increase from 1249 to 1800 m and then decrease to 1599 m northwestward (Table S1). Four samples are located on the top and the southern slope (the southern part), and the rest four samples are located on the northern slope (the northern part; Figure 4).

AHe dating was conducted in $^{40}Ar/^{39}Ar$ and (U-Th)/He geochronology laboratory, Institute of Geology and Geophysics, Chinese Academy of Sciences. After the standard rock crushing and heavy liquid separation procedures, five relatively euhedral, intact, and transparent apatite grains free of visible inclusions and internal fractures were selected and measured under a microscope. Due to the limited quality of apatite grains from these samples, some translucent or slightly broken grains or grains with small inclusions were still picked, whose impacts on AHe ages are discussed in the section of results. After measurement of the length and width, each grain was then wrapped in a 1 mm × 1 mm platinum (Pt) capsule and loaded on a drilled oxygen-free copper disk. Helium measurement was performed using a fully automatic helium extraction system called Alphachron MK II (Australian Scientific Instrument Pty Limited). After helium extraction, Pt wrapped grains were transferred to Savillex PFA vials and spiked with ^{230}Th-^{235}U solution with known concentration. All the spiked solutions were measured on a Thermo Fisher X-Series II inductively coupled plasma mass spectrometry. Age calculation was conducted by a java-based program named Helioplot [54] and corrected for alpha ejection following the procedure of Gautheron et al. [55]. MK-1 apatite [56, 57] was used as a reference standard to verify the analytical procedure. A detailed analytical procedure was described by Wu et al. [56, 58].

AHe thermal history modeling was carried out using HeFty software (1.9.0 version; [59]). Measured single-grain AHe ages, the content of U and Th, and grain size (Rs) were imported. The radiation damage accumulation and annealing model [60] was adopted. Monte Carlo method was chosen as the searching method, and 100,000 path was tried in each modeling. The present-day temperature was set as 10 ± 10°C. The start time and temperature were set as 140–120 Ma and 140–120°C, much older than the oldest single-grain AHe age and higher than the AHe closure temperature, respectively. Notably, the analysis of AHe thermal history modeling results in this study was

Figure 3: Field photos of the sampled granitic and gneissic plutons.

mainly based on the general trend of the acceptable and good fit paths, despite that the best-fitting and weighted lines were also presented which served as the reference frame.

4. Results

4.1. AHe Ages. Corrected single-grain AHe ages of eight samples range from 152.3 ± 8.0 to 30.4 ± 1.6 Ma (Table S2). They present large intrasample dispersions. The intrasample dispersion usually arises from the analysis of the broken crystals [61], the presence of mineral and fluid inclusions [62], the variation in grain sizes [63], the radiation damage [60, 64], and the zonation of U-Th [65]. Specifically, AHe ages of grains D18-11-A1, D18-11-A5, and D18-23-A4 are anomalously younger than those of other grains in each sample (Table S2). This is probably owing to the breakage of these three grains (Figures 5(a) and 5(h)) as demonstrated in Brown et al. [61]. Grains D18-12-A4, D18-14-A2, D18-14-A5, D18-16-A3, and D18-23-A5 are translucent under the microscope (Figures 5(b)–5(d) and 5(h)). Their AHe ages are significantly older than the other grains in each sample (Table S2). Undetected mineral or fluid inclusions may exist in these three grains [62]. Apart from the breaking of grains and mineral or fluid inclusions, intrasample dispersion of single-grain AHe ages also could be related to grain size [63] and radiation damage [60, 64]. To explore the possible effects of grain size and radiation damage, AHe raw age versus Rs (grain spherical equivalent radius) and eU (effective uranium; Table S2) was plotted for the rest single grains (Figure 6). Samples D18-12, D18-14, and D18-24 display a roughly positive correlation between single-grain AHe ages and Rs (Figure 6(a)). Dispersions in these three samples may be partially caused by the differences of grain sizes. Samples D18-11, D18-17, and D18-22 show a roughly positive correlation between single-grain AHe ages and eU (Figure 6(b)). These three samples may be slightly affected by the radiation damage effect. Furthermore, samples D18-11 and D18-17 are mylonitic granite and granitic gneiss, respectively. Their intrasample dispersions may be also resulted from the lattice damage formed during the deformation, similarly

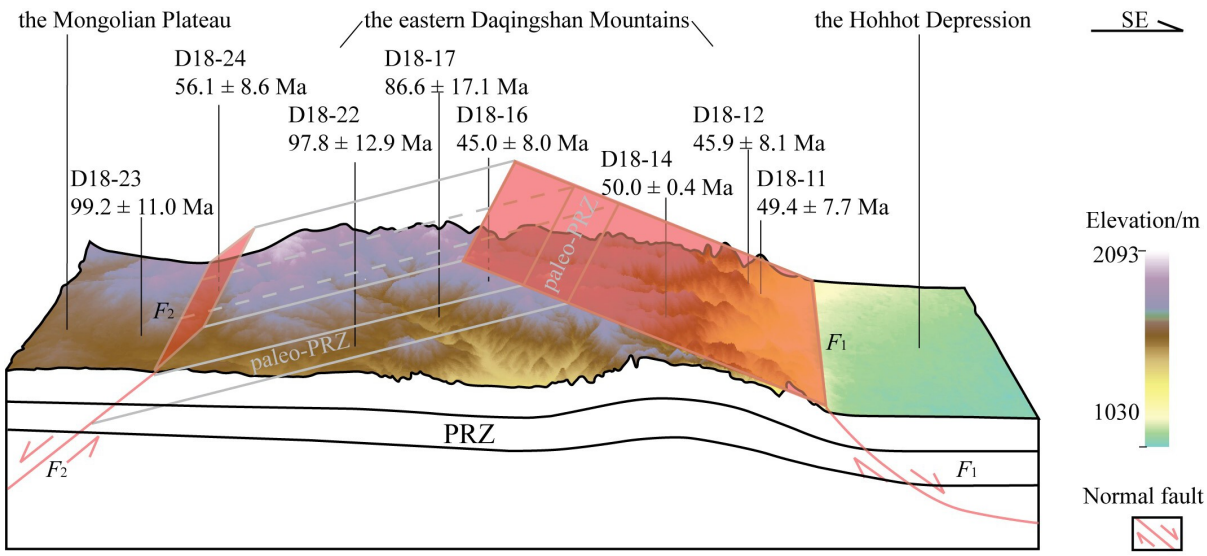

Figure 4: DEM slice along the Kuisu-Dalanqi transect with the speculative model of the Late Paleocene–Eocene extension, tilting, and differential denudation in the eastern Daqingshan Mountains. Sample position and mean corrected AHe ages are indicated. PRZ indicates the AHe partial retension zone.

as the radiation damage [64]. In addition, single-grain AHe ages of samples D18-16 and D18-23 show no clear correlation between Rs and eU (Figure 6). Their dispersions are probably a combined effect of Rs [63], eU [60, 64], undetected inclusions [62], and U-Th inhomogeneity [65]. Nevertheless, excluding the above eight outliers, the relative standard deviations of the eight samples for corrected AHe ages are all ≤20% (11%–20%), satisfied with the criteria to calculate mean AHe ages [66].

Eight samples yield mean corrected AHe ages ranging from 99.2 ± 11.0 to 45.0 ± 8.0 Ma (Table S2). They could be divided into two groups: (1) three in the first group with almost the same age of Late Cretaceous (99.2 ± 11.0 to 86.6 ± 17.1 Ma) and dispersed over an elevation range from 1730 to 1599 m; (2) five in the second group with almost the same age of Late Paleocene–Early Eocene (56.1 ± 8.6 to 45.0 ± 8.0 Ma) distributed over a vertical range of 1800–1249 m (Figure 7). AHe ages in the first group are prominently older than those in the second group (Figure 7). Moreover, three samples in the first group are all distributed in the northern part of the eastern Daqingshan Mountains (Figure 4). Four samples in the second group are spread in the southern part of the eastern Daqingshan Mountains, with the other one in the northern part (Figure 4).

4.2. AHe Thermal History Modeling Results. Constraints were set according to the geological conditions of the eastern Daqingshan Mountains as well as that of the Hohhot Depression from the viewpoint of basin-mountain coupling. For samples with the Late Cretaceous AHe ages, one constraint was roughly set as 100–65 Ma on time and 80–40°C (AHe PRZ; [67]) on temperature given the absence of the Late Cretaceous strata in the eastern Daqingshan Mountains (Figure 2). These samples were speculated to cool rapidly through the AHe PRZ during the Late Cretaceous. For samples with the Late Paleocene–Early Eocene AHe ages, the Tertiary sedimentation in the Hohhot Depression was also taken into consideration, assuming the provenance of the Cenozoic sediments in the Hohhot Depression was mainly derived from the eastern Daqingshan Mountains. However, considering the divergence about the Tertiary bottom strata in the Hohhot Depression (Figure 2): the Miocene Wuyuan Fm [24] or the Late Paleocene–Early Eocene Wulate Fm [33], constraints were separately set in two scenarios to explore the most likely time-temperature paths. In scenario 1, samples were speculated to cool across the bottom limit of the AHe PRZ during the Late Cretaceous and the upper limit of the AHe PRZ during the Miocene. Two constraints were roughly set: 100–65 Ma on time and 80–40°C on temperature and 20–5 Ma on time and 60–0°C (60°C is used to generally represent the middle of the AHe PRZ) on temperature. In scenario 2, samples were speculated to cool rapidly through the AHe PRZ during the Late Paleocene–Early Eocene, and only one constraint was set as 60–45 Ma on time and 80–40°C on temperature.

For samples with the Late Cretaceous AHe ages, all the thermal history modeling obtains acceptable (ACC) and good fit paths. The GOF (good of fitness) values range from 0.99 to 0.18. The thermal history modeling results mainly indicate cooling through the AHe PRZ during the Late Cretaceous (Figure 8). For samples with the Late Paleocene–Early Eocene AHe ages, only thermal history modeling of D18-11, D18-14, and D18-24 gets both acceptable and good fit paths, but all acquires abundant acceptable paths. The GOF values range from 1.00 to 0.14. Notably, acceptable paths obtained in scenario 2 outnumber those in scenario 1 (Figure 9). The thermal history modeling results acquired in scenario 2 demonstrate cooling through the AHe PRZ during the Late Paleocene–Eocene (Figures 9(a2)–9(e2)). Moreover, the thermal history modeling results acquired in scenario 1 show

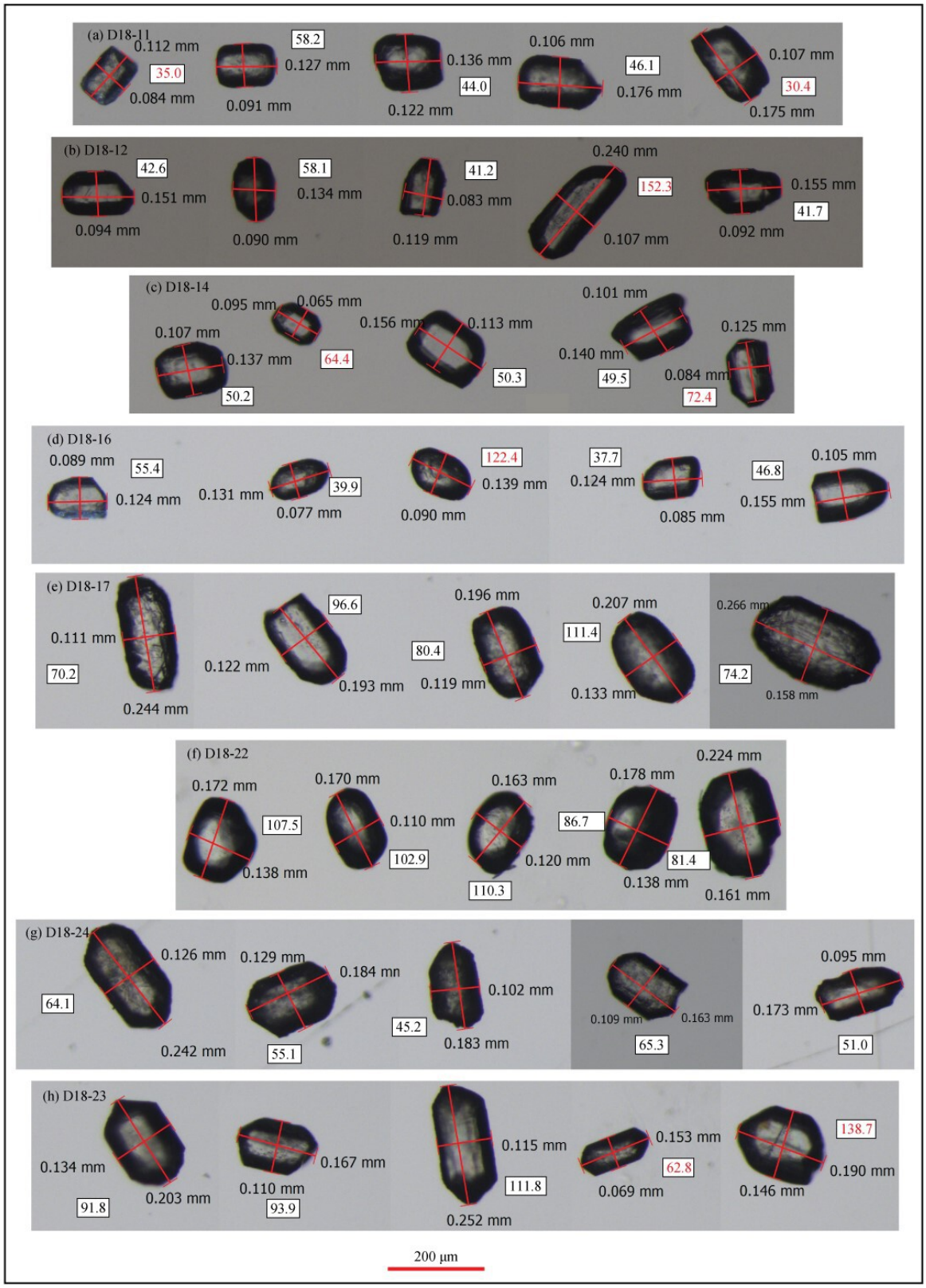

FIGURE 5: Photomicrographs of the analyzed apatite grains under reflected light with an indication of their sizes and corrected single-grain AHe ages (Ma) in the rectangle, among which AHe ages in red indicate the outliers.

cooling into the AHe PRZ during the Late Cretaceous and from the AHe PRZ to above the AHe PRZ during the Late Paleocene–Eocene but not the Miocene (Figures 9(a1)–9(e1)). To conclude, the AHe data obtained in this study are

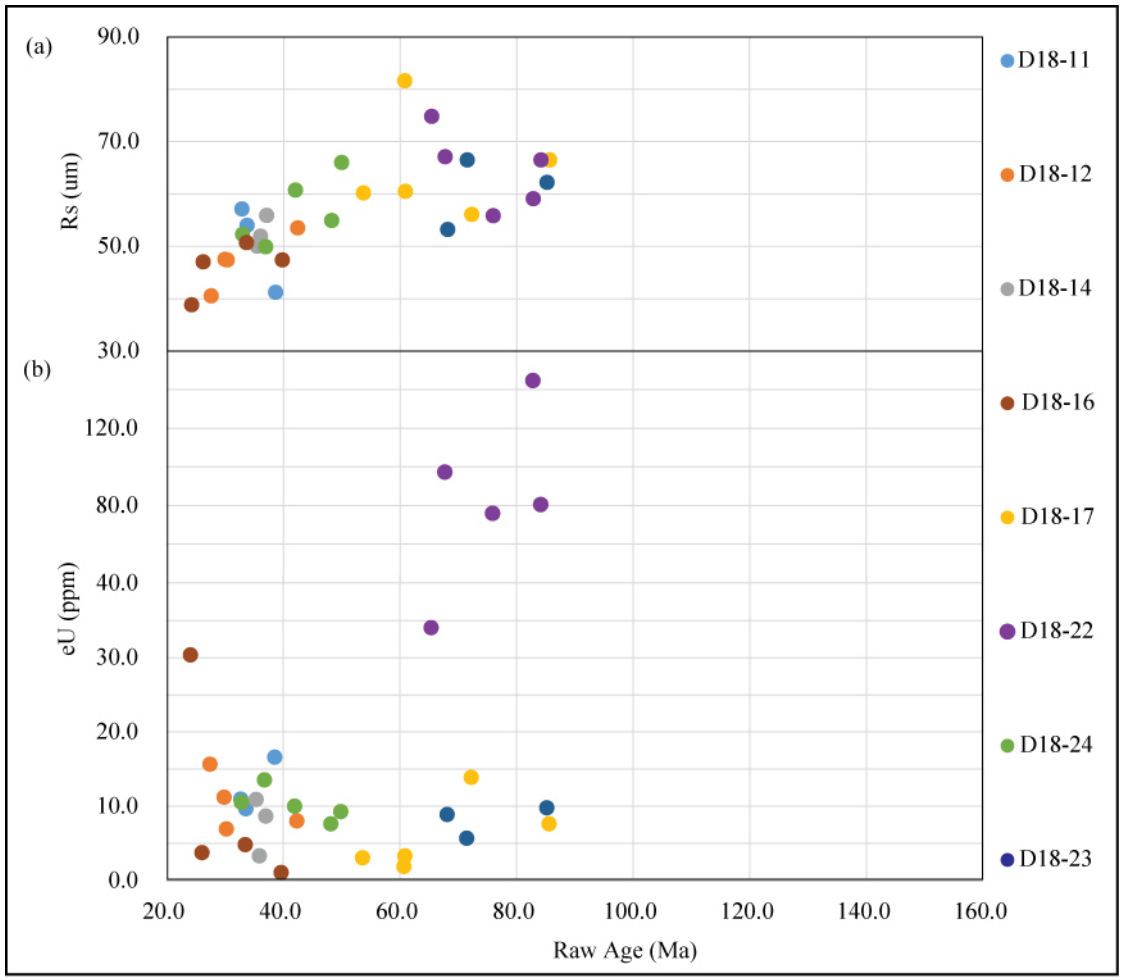

Figure 6: Relationship between raw single-grain AHe ages and Rs as well as eU.

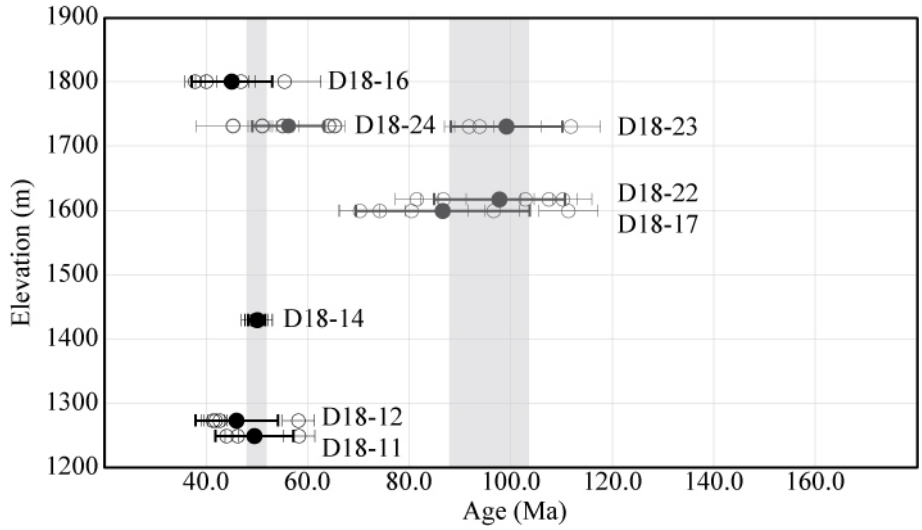

Figure 7: AHe age-elevation relationship in the eastern Daqingshan Mountains. Black and dark gray circles indicate samples in the southern and northern parts of the eastern Daqingshan Mountains, respectively; solid circles indicate the mean corrected AHe ages of each sample; hollow circles indicate the single-grain corrected AHe ages of each sample. Light gray rectangles show the overlap of the mean corrected AHe ages within the standard deviations.

in better agreement with scenario 2, and the Late Paleocene–Eocene cooling in the eastern Daqingshan Mountains is demonstrated in both scenarios (Figure 9).

5. Discussion

AHe thermal history modeling results indicate two periods of cooling after the Early Cretaceous denudation and cooling event [45–49]: the Late Cretaceous and the Late Paleocene–Eocene (Figure 10).

5.1. The Late Cretaceous Denudation/Cooling Event and Its Tectonic Implications. The Late Cretaceous cooling in the northern part of the eastern Daqingshan Mountains, displayed by AHe thermal history modeling results, is in accord with the ca. 100–90 Ma cooling event in the southern part of the eastern Daqingshan Mountains revealed by AFT thermal history modeling results (Figure 10; [34, 35]). This temporal overlap indicates widespread cooling in the eastern Daqingshan Mountains during the Late Cretaceous. Sedimentologically, the Upper Cretaceous is neither exposed in the eastern Daqingshan Mountains nor in the Hohhot Depression. The eastern Daqingshan Mountains and the Hohhot Depression around the northeastern margin of the Ordos Block might experience overall uplift and denudation at that time. Notably, the Tertiary basal strata in the Hohhot Depression directly overlie the Lower Cretaceous unconformably. Altogether, the wholescale denudation probably occurred at least during the Late Cretaceous.

Regionally, the Late Cretaceous denudation and cooling event is also reported in the Ordos Basin [68] and other peripheral mountains: the Langshan and Seertengshan Mountains, northwestern margin [28, 29]; the western Daqingshan Mountains, northern margin [30]; the north-central part of the Shanxi Rift Systems, eastern margin [69]; the Taibai Mountains, southeastern margin [70]; and the Helanshan Mountains, western margin [23]. To the east of the Ordos Block, the Yanshan Mountains [71, 72], the Taihangshan Mountains [73, 74], the Jiaodong Peninsula [75, 76], and Yanji area [77] in the eastern part of the NCC experienced denudation and cooling during the Late Cretaceous as well. The abovementioned Late Cretaceous denudation and cooling events are temporally overlapped with the denudation and planation that leads to the formation of the Beitai Planation Surface preserved in the Taihangshan Mountains, the timing of which was constrained by the youngest known stratum subjected to planation (ca. 97 Ma) and the oldest known stratum in the overlying weathering crust (ca. 54 Ma) [78]. Meanwhile, the weathering crust in the bottom of the Bohai Bay Basin (BBB) underlying the Paleocene Lower Kongdian Fm. also implies Late Cretaceous denudation therein [79, 80]. Consequently, the Late Cretaceous denudation is probably widespread in both the western and eastern parts of the NCC. It agrees well with the prevailing absence of the Upper Cretaceous across the NCC. Such a regional event is probably reflective of the overall uplift of the NCC and concomitant planation during the Late Cretaceous. It temporally corresponds to the late stage of the "Yanshan Orogeny" in East Asia which is featured by weak NW-SE compressional deformations and basin inversion (100–83 Ma; [81, 82]). The intensification of the westward subduction of the Izanagi-Pacific Plate under East Asia during the early Late Cretaceous and the collision between the Okhotomorsk Block and the East Asian around ca. 100 Ma were probably responsible [3, 83].

5.2. The Late Paleocene–Eocene Denudation/Cooling Event and Its Tectonic Implications

5.2.1. The Late Paleocene–Eocene Denudation/Cooling Event. Thermal history modeling results of samples with the Late Paleocene–Early Eocene AHe ages indicate the Late Paleocene–Eocene cooling in the eastern Daqingshan Mountains (Figure 9). Although the relatively small elevation range (ca. 500–600 m) of samples is insufficient to exhume the break, the Late Paleocene–Early Eocene AHe ages are overlapped within the standard deviations and do not show any trend of a slow denudation in the age-elevation correlation (Figure 7), suggesting the elevation range represent a part of rapid denudation. Besides, previous AFT results indeed displayed Cenozoic cooling signature before Miocene in the southern part of the eastern Daqingshan Mountains (Figure 10; [35]). All in all, rapid denudation and cooling during the Late Paleocene–Eocene in the eastern Daqingshan Mountains is preferred in this study.

Notably, only one sample with the Late Paleocene–Early Eocene AHe age is distributed in the northern part of the eastern Daqingshan Mountains (Figure 4), suggesting relatively weak denudation and cooling therein than that in the southern part of the eastern Daqingshan Mountains during the Late Paleocene–Eocene.

5.2.2. The Initiation of the Extension Around the Northeastern Margin of the Ordos Block During the Cenozoic. Several fault cliffs of the normal fault F_1 are outcropped along the southern piedmont of the eastern Daqingshan Mountains with relatively steep dips of ca. $\angle 50°$ [16]. Three sets of striations on the fault cliffs [16] suggest multistage of extension. The syn-tectonic Cenozoic strata in the Hohhot Depression demonstrated by the geophysical data [25] also correspond to the multistage of activities of the normal fault F_1. In particular, the basal conglomerate rocks of the Tertiary strata uncomfortably overlying the Lower Cretaceous suggest the timing of initial extension between the eastern Daqingshan Mountains and the Hohhot Depression to be Miocene or Late Paleocene–Early Eocene [24, 33].

Notably, the differential denudation during the Late Paleocene–Eocene in the eastern Daqingshan Mountains is probably dominated by the normal fault F_1, indicated by the relationship between the pattern of AHe ages and the normal faults F_1 and F_2. AHe ages show a younger-older-younger-older pattern from the footwall of F_1 to the hanging wall of F_2 (Figure 4) along the transect, conforming to the tilting and following differential denudation caused by the activities of the normal faults F_1 and F_2. Generally, rocks in the fault zone of the normal fault would be

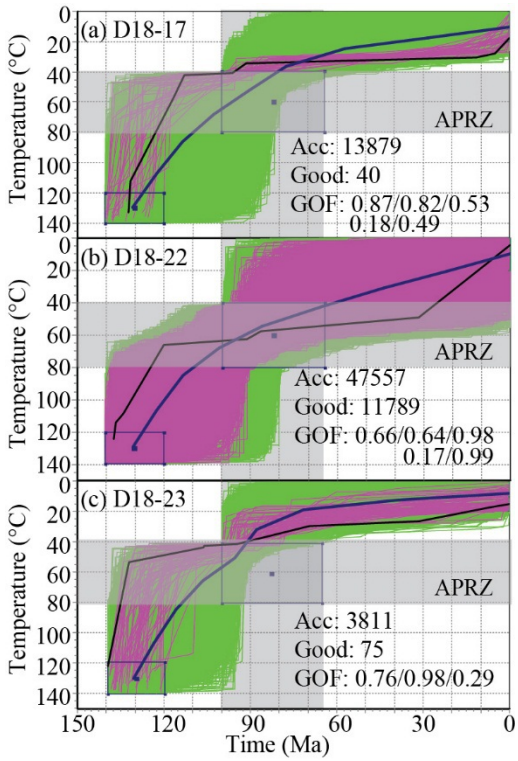

Figure 8: AHe thermal history modeling results of samples with the Late Cretaceous AHe ages. Blue rectangles indicate constraints. Green and magenta curves indicate the acceptable and good fit paths, respectively; black and bold curve indicates the best fit model; blue and bold curve indicates the weighted mean path. Semitransparent vertical gray band indicates the Late Cretaceous cooling event. APRZ, AHe partial retention zone.

differentially exhumed along with the downward movement of the hanging wall, whereas rocks on the footwall may also suffer from differential denudation caused by the tilting of the fault plane which is usually brought about in faults with steep dips (Figure 4). Samples D18-11 and D18-12 are in the fault zone of F_1. Samples D18-14 to D18-16 and D18-24 are on the footwall of F_1 and F_2, respectively. The rapid cooling of samples D18-11 to D18-12 and D18-14 to D18-16 from below the AHe PRZ to above the AHe PRZ is probably caused by the downward movement of the hanging wall and the tilting of the footwall of F_1 with subsequent denudation (Figure 4). As a result, their AHe ages are similarly younger, and AHe thermal history modeling results show rapid cooling during the Late Paleocene–Eocene (Figures 9(a)–9(d)), which might represent the timing of the activity of F_1. However, the activity of the normal fault F_2 might not be as intensive as F_1, as only one sample D18-24 was denudated from the AHe PRZ to above the AHe PRZ by the downward movement of the hanging wall of F_2 (Figure 4) and kept the record of previous Late Cretaceous denudation and cooling (Figure 9(e)). Whereas samples D18-17 and D18-22, far away from F_1 and F_2, might be hardly influenced by the activity of both normal faults (Figure 4). Thus, their AHe ages are similarly older and only keep records of previous Late Cretaceous denudation and cooling (Figure 8). As with D18-23, it is on the hanging wall of F_2 and more far away from F_1, the only record of previous Late Cretaceous denudation and cooling is retained as well (Figure 8). To conclude, the spatial pattern of AHe ages across the eastern Daqingshan Mountains is consistent with the differential denudation induced by the faulting and tilting of the normal faults F_1 and F_2.

On these grounds, the differential denudation during the Late Paleocene–Eocene in the eastern Daqingshan Mountains shares the same dynamics with the syn-tectonic Tertiary strata in the Hohhot Depression. Moreover, it is temporally overlapped with the Wulate Fm. Correspondingly, the normal fault F_1 was probably initiated during the Late Paleocene–Eocene and triggered the tilting and resultant differential denudation in the eastern Daqingshan Mountains and the subsidence of the Hohhot Depression. The eroded materials were probably deposited in the nearby Hohhot Depression and formed the syn-tectonic deposition of the Wulate Fm. The normal fault F_2 was also reactivated to accommodate the mass movement [53]. The embryo of the current mountain-basin system around the northeastern margin of the Ordos Block was then shaped (Figure 4).

5.2.3. Tectonic Implications. Temporal and dynamic coupling between the Late Paleocene–Eocene denudation in the eastern Daqingshan Mountains and the syn-tectonic deposition of the Wulate Fm. in the Hohhot Depression suggests that extension probably had already occurred around the northeastern margin of the Ordos Block during the Late Paleocene–Eocene. Regionally, Paleocene–Eocene denudation and cooling event in the Lvliangshan, Huoshan, Zhongtiaoshan, Huashan, and Taibai Mountains [19, 20, 84–87] and Paleocene–Eocene deposition in the Weihe-Lingbao Basins [18] are also reported, together with the compilation of AFT and AHe ages centering at 38 Ma [19], indicating widespread Eocene extension in the Shanxi Rift System, eastern and southeastern margin of the Ordos Block (Figure 1). The Cenozoic extension and syn-tectonic deposition also initiated during the Eocene in the Yinchuan Basin, western margin of the Ordos Block ([22]; Figure 1). The syn-tectonic Wulate Fm. in the Linhe Depression of the Hetao Basin [26] and cooling in the Langshan [28] and Seertengshan Mountains [29] around the northwestern margin and the cooling in the western Daqingshan Mountains [30, 31] around the northern margin of the Ordos Block occurred in the Late Paleocene–Eocene as well (Figure 1). More widely, the Bohai Bay Basin to the east of the Ordos Block suffered from intensive rifting and deposition during the Paleocene–Early Eocene ([88–90], along with dispersed cooling around the Bohai Bay Basin, including the Yanshan Mountains, the Taishan Mountains, the Jiaodong Peninsula, the Subei Basin, the Hefei Basin, the Qinling–Dabie Mountains, and the Taihang Mountains (58, 71, 74 and references therein, 91–97; Figure 1). Notably, the orientation of the aforesaid Eocene extension across the NCC is similarly NW-SE [12, 16]. Striations on the fault cliffs of the normal fault F_1 in the eastern Daqingshan Mountains also indicate nearly NW-SE extension in the

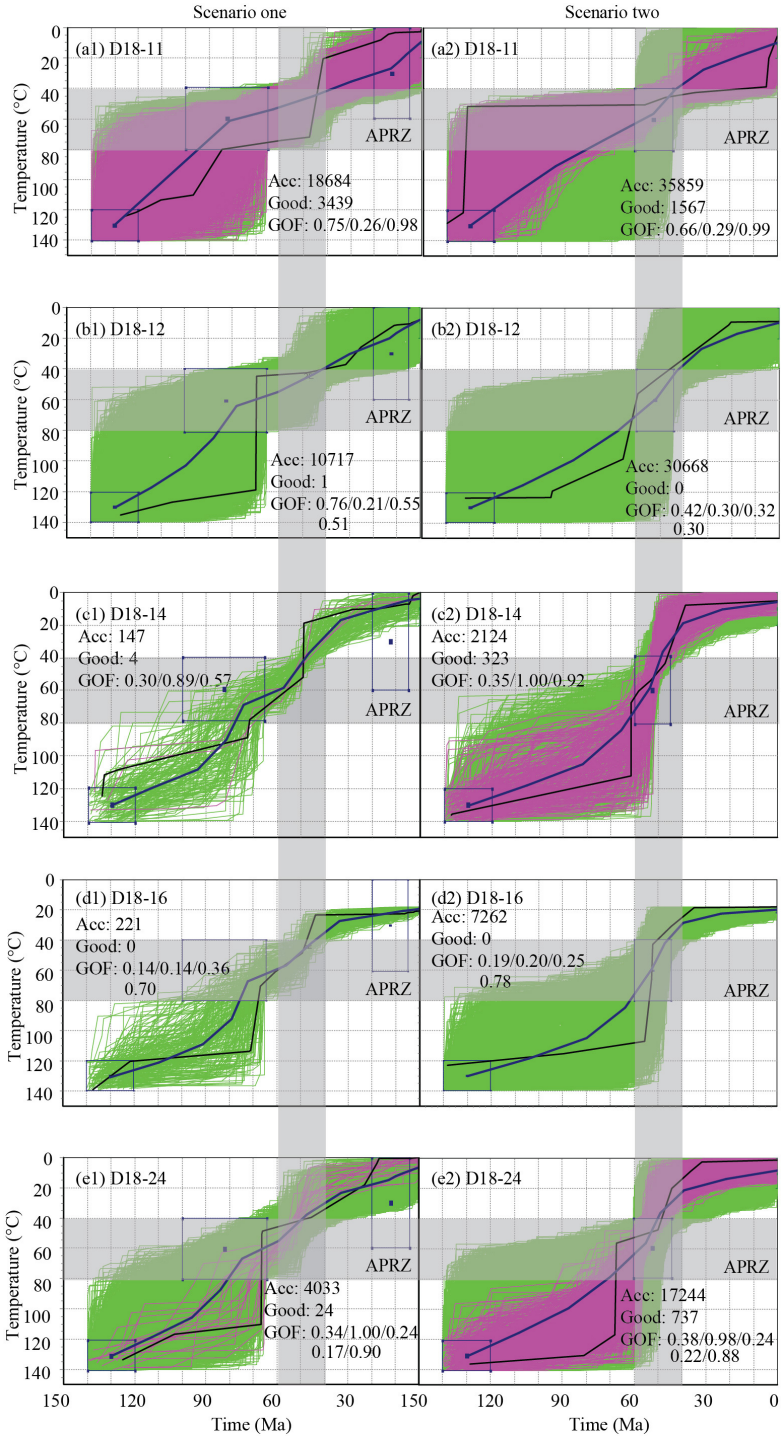

FIGURE 9: AHe thermal history modeling results of samples with the Late Paleocene–Early Eocene AHe ages. Blue rectangles indicate constraints. Green and magenta curves indicate the acceptable and good fit paths, respectively; black and bold curve indicates the best fit model; blue and bold curve indicates the weighted mean path. Semitransparent vertical gray band indicates the Late Paleocene–Eocene cooling event. APRZ, AHe partial retention zone.

early stage [16], suggesting that the eastern Daqingshan Mountains is controlled by a likely unified geodynamics mechanism within the NCC during the Eocene.

Geodynamically, the Izanagi-Pacific plate to the east was subducted along the eastern margin of East Asia during the Cenozoic [3, 5, 98, 99]. The subduction rate reduced significantly with the direction changing from N-NNW to NW about 50 Ma ago [3] or with the transition of the subducted plate from the Izanagi plate to the Pacific plate in the process of the ridge subduction around 56–46 Ma [5]. The Eocene extension across the NCC is coincided kinematically and temporally with the northwestward

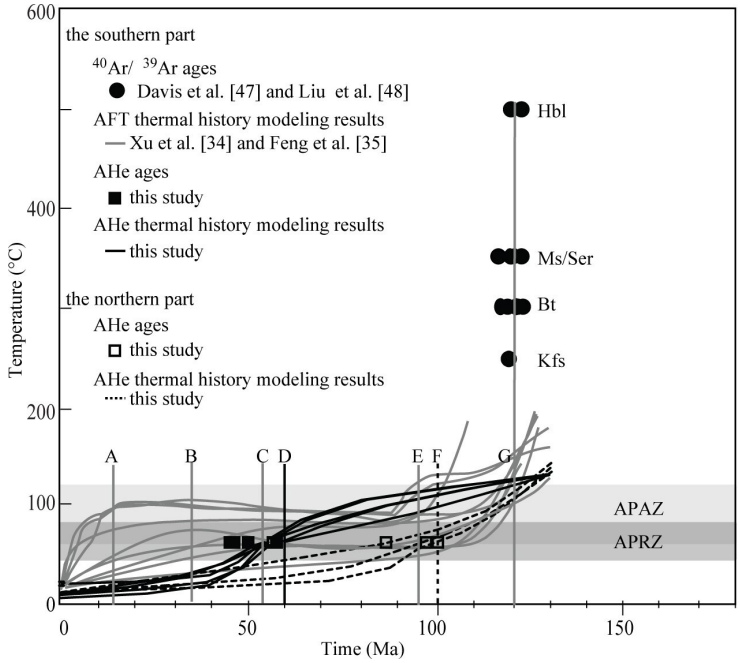

Figure 10: Thermochronological T-t paths in the eastern Daqingshan Mountains. Gray straight-lines A, B, C, E, and G indicate the Miocene, Oligocene, Eocene, Late Cretaceous, and Early Cretaceous cooling events in the southern part of the eastern Daqingshan Mountains shown by the AFT thermal history modeling results from References 34, 35 and the $^{40}Ar/^{39}Ar$ ages from References 47, 48. Black straight-line D and black dotted straight-line F indicate the Late Paleocene–Eocene and Late Cretaceous cooling events in the southern and northern parts of the eastern Daqingshan Mountains, respectively, shown by the weighted mean paths from the AHe thermal history modeling results in this study. Abbreviations: Hbl, hornblende; Ser, sericite; Ms, muscovite; Bt, biotite; Kfs, k-Feldspar; APAZ, AFT partial annealing zone; APRZ, AHe partial retention zone.

subduction of the Izanagi-Pacific plate and the decrease in subduction rate. Dynamically, the reduction of the compressive stress triggered by the deceleration of the subduction also agrees with the extension in the overlying plate. Therefore, the subduction of the Izanagi-Pacific plate probably plays a major role in the Eocene extension across the NCC. However, the continued India-Asia collision to the southwest substantially influenced the Cenozoic evolution of East Asia (1, 82 and references therein, 100) as well. The Eastern Kunlun, Altyn, Qilian, and Western Qinling Mountains were rapidly denudated around 54–50 Ma with sedimentation in adjacent basins and thrusting or strike slipping of the bounded faults [101–106] in the northern and northeastern Tibet Plateau, despite that substantial surface uplift to high elevations of the Kunlun Mountains and the northern Tibet probably occurred after ca. 25 Ma (9 and references therein). The far-field effect of the India-Asia collision is probably almost synchronously transmitted northeastward to the NCC, and the resulting eastward lateral mantle flow may contribute to the widespread Cenozoic extension in eastern China [107]. Accordingly, the influence of the India-Asia collision could not be ignored.

6. Conclusions

AHe ages are reported for the first time on eight granitic and gneissic samples across the eastern Daqingshan Mountains around the northeastern margin of the Ordos Block, western NCC. Eight mean corrected AHe ages range from 99.2 ± 11.0 to 45.0 ± 8.0 Ma. Specifically, four mean corrected AHe ages in the southern part of the eastern Daqingshan Mountains are overlapped within the standard deviations between 50.0 ± 0.4 and 45.0 ± 8.0 Ma. However, three mean corrected AHe ages in the northern part of the eastern Daqingshan Mountains are obviously older of 99.2 ± 11.0 to 86.6 ±17.1 Ma with the rest one of 56.1 ± 8.6 Ma. Along the sampled transect, mean corrected AHe ages show a younger-older-younger-older pattern which correlates with the normal faults F_1 and F_2. AHe thermal history modeling results demonstrate widespread cooling during the Late Cretaceous and differential cooling during the Late Paleocene–Eocene in the eastern Daqinghsan Mountains. The Late Cretaceous cooling is probably resulted from contemporaneous wholescale uplift and denudation of the NCC. The Late Paleocene–Eocene differential cooling and the relationship between the spatial pattern of AHe ages and the normal faults are probably caused by the activity of the normal faults, accompanied by the titling and differential denudation of the eastern Daqingshan Mountains. Regional comparative analysis indicates that the Late Paleocene–Eocene extension occurred widely across the NCC and is temporally, kinematically, and dynamically coupled with the subduction of the Izanagi-Pacific plate. The subduction of the Izanagi-Pacific plate is probably dominantly responsible for this regional extension event, whereas the effect of the India-Asia collision could not be neglected.

Data Availability

The data used to support the findings of this study are included within the supplementary materials.

Conflicts of Interest

The authors declare no conflict of interest regarding this manuscript.

Acknowledgments

This work was financially supported by Sichuan Elementary Education Research Centre (No. 20SZSJYZ-04), Sichuan Science and Technology Program (No. 2022NSFSC1022), and the Talent Introduction Project of Xi Hua University (No. RZ2000002858).

Supplementary Materials

The supplementary materials contain files of 2 tables. Table S1: AHe sample information in the eastern Daqingshan Mountains. Table S2: AHe data in the eastern Daqingshan Mountains.

References

[1] A. Yin, "Cenozoic Tectonic evolution of Asia: A preliminary synthesis," *Tectonophysics*, vol. 488, nos. 1–4, pp. 293–325, 2010.

[2] P. Z. Zhang, H. P. Zhang, W. J. Zheng, D. W. Zheng, W. T. Wang, and Z. Z.Q, "Cenozoic Tectonic evolution of Continental Eastern Asia," *Seismic and Geology*, vol. 36, no. 3, pp. 574–583, 2014.

[3] C. J. Northrup, L. H. Royden, and B. C. Burchfiel, "Motion of the Pacific plate relative to Eurasia and its potential relation to Cenozoic extension along the Eastern margin of Eurasia," *Geology*, vol. 23, no. 8, p. 719, 1995.

[4] N. M. Wright, M. Seton, S. E. Williams, and R. D. Müller, "The late Cretaceous to recent Tectonic history of the Pacific ocean Basin," *Earth-Science Reviews*, vol. 154, March, pp. 138–173, 2016.

[5] J. T.-J. Wu and J. Wu, "Izanagi-Pacific ridge Subduction revealed by a 56 to 46 ma Magmatic gap along the northeast Asian margin," *Geology*, vol. 47, no. 10, pp. 953–957, 2019.

[6] C. Wang, X. Zhao, Z. Liu, et al., "Constraints on the early uplift history of the Tibetan plateau," *Proceedings of the National Academy of Sciences*, vol. 105, no. 13, pp. 4987–4992, 2008.

[7] C. S. Wang, J. G. Dai, X. X. Zhao, et al., "Outward-growth of the Tibetan plateau during the Cenozoic: A review," *Tectonophysics*, vol. 621, May, pp. 1–43, 2014.

[8] L. Ding, M. Qasim, I. A. K. Jadoon, et al., "The India–Asia collision in North Pakistan: Insight from the U–PB Detrital Zircon provenance of Cenozoic foreland Basin," *Earth and Planetary Science Letters*, vol. 455, December, pp. 49–61, 2016.

[9] L. Ding, P. Kapp, F. Cai, et al., "Timing and mechanisms of Tibetan plateau uplift," *Nature Reviews Earth & Environment*, vol. 3, no. 10, pp. 652–667, 2022.

[10] State Seismology Bureau, *Peripheral Active Fault System around the Ordos*, Seismological Press, Beijing, 1988.

[11] Y. Q. Zhang, J. L. Mercier, and P. Vergély, "Extension in the Graben systems around the Ordos (China), and its contribution to the extrusion Tectonics of South China with respect to Gobi-Mongolia," *Tectonophysics*, vol. 285, nos. 1–2, pp. 41–75, 1998.

[12] Z. Yueqiao, M. Yinsheng, Y. Nong, S. Wei, and D. Shuwen, "Cenozoic Extensional stress evolution in North China," *Journal of Geodynamics*, vol. 36, no. 5, pp. 591–613, 2003.

[13] Y. Q. Zhang, C. Z. Liao, W. Shi, and B. Hu, "Neotectonic evolution of the peripheral zones of the Ordos basin and Geodynamic setting," *Geological Journal of China Universities*, vol. 12, pp. 285–297, 2006.

[14] Y. Q. Zhang, W. Shi, and S. W. Dong, "Neotectonics of North China: Interplay between far-field effect of India-Eurasia collision and Pacific Subduction related deep-seated Mantle Upwelling," *Acta Geologica Sinica*, vol. 93, no. 5, pp. 971–1001, 2019.

[15] Q. D. Deng, S. P. Chen, W. Min, G. Z. Yang, and D. W. Reng, "Discussion on Cenozoic Tectonics and Dynamics of the Ordos block," *International Journal of Rock Mechanics and Mining Sciences*, vol. 5, no. 3, pp. 13–21, 1999.

[16] W. Shi, S. W. Dong, and J. M. Hu, "Neotectonics around the Ordos block, North China: A review and new insights," *Earth-Science Reviews*, vol. 200, January, p. 102969, 2020.

[17] J. Liu, P. Zhang, R. O. Lease, et al., "Eocene Onset and late Miocene acceleration of Cenozoic Intracontinental extension in the North Qinling range–Weihe Graben: Insights from Apatite fission track Thermochronology," *Tectonophysics*, vol. 584, January, pp. 281–296, 2013.

[18] S. Fan, T. Zhang, S. Chen, and R. Li, "New findings regarding the fen-wei Graben on the southeastern margin of the Ordos block: Evidence from the Cenozoic sedimentary record from the Borehole," *Geological Journal*, vol. 55, no. 12, pp. 7581–7593, 2020. https://onlinelibrary.wiley.com/toc/10991034/55/12.

[19] C. Clinkscales, P. Kapp, S. Thomson, et al., "Regional Exhumation and Tectonic history of the Shanxi rift and Taihangshan, North China," *Tectonics*, vol. 40, no. 3, 2021.

[20] P. Su, H. He, X. Tan, Y. Liu, F. Shi, and E. Kirby, "Initiation and evolution of the Shanxi rift system in North China: Evidence from low temperature Thermochronology in a plate reconstruction framework," *Tectonics*, vol. 40, no. 3, 2021.

[21] J. H. Liu, P. Z. Zhang, D. W. Zheng, et al., "Pattern and timing of late Cenozoic rapid Exhumation and uplift of the Helan mountain, China," *Science China: Earth Science*, vol. 40, no. 1, pp. 50–60, 2010.

[22] X. B. Liu, J. M. Hu, W. Shi, H. Chen, and J. Y. Yan, "Palaeogene–Neogene sedimentary and Tectonic evolution of the Yinchuan Basin, Western North China Craton," *International Geology Review*, vol. 62, no. 1, pp. 53–71, 2020.

[23] G. Z. Shi, C. B. Shen, M. Zattin, H. Wang, C. Q. Yang, and C. Liang, "Late Cretaceous-Cenozoic Exhumation of the Helanshan mt range, Western Ordos fold-thrust belt, China: Insights from structural and Apatite fission track analyses,"

Journal of Asian Earth Sciences, vol. 176, June, pp. 196–208, 2019.

[24] S. L. Gao, *Research about Geological Conditions of Shallow Gas (Biogenic Gas) Accumulation in Hetao Basin*, Northwest University, Xi`an, 2007.

[25] S. Y. Feng, B. J. Liu, and J. F. Ji, "The survey on fine Lithospheric structure beneath Hohhot-Baotou Basin by deep seismic reflection profile," *Chinese Journal of Geophysics*, vol. 58, no. 4, pp. 1158–1168, 2015.

[26] S. Fu, J. Fu, J. Yu, et al., "Petroleum geological features and exploration prospect of Linhe depression in Hetao Basin, China," *Petroleum Exploration and Development*, vol. 45, no. 5, pp. 803–817, 2018.

[27] L. X. Feng, R. W. Brown, B. F. Han, et al., "Thrusting and Exhumation of the Southern Mongolian plateau: Joint Thermochronological constraints from the Langshan mountains, Western inner Mongolia, China," *Journal of Asian Earth Sciences*, vol. 144, August, pp. 287–302, 2017.

[28] X. Cui, Q. Zhao, J. Zhang, et al, "Late Cretaceous-Cenozoic multi-stage Denudation at the Western Ordos block: Constraints by the Apatite fission track dating on the Langshan," *Acta Geologica Sinica*, vol. 92, no. 2, pp. 536–555, 2018.

[29] X. C. Yang, "Uplift process of the Western section of Yinshan from Mesozoic to Cenozoic period and its geological implications [Phd thesis]," , Chinese Academy of Geological Sciences, Beijing, 2018.

[30] Z. H. Wu and Z. H. Wu, "Uplift history of the Daqing mountain since the late Cretaceous," *Acta Geoscientia Sinica*, vol. 24, no. 3, pp. 205–210, 2003.

[31] J. L. Zhou, Y. H. Li, W. Han, et al., "Cretaceous–Neogene Exhumation of the Daqing shan, North China constrained by Apatite fission track Thermochronology," *Journal of Earth Science*, 2021. https://kns.cnki.net/kcms/detail/42.1788.P.20210723.0916.002.html.

[32] H. Peng, J. Q. Wang, C. Y. Liu, L. Huang, and M. Zattin, "Mesozoic Exhumation and ca. 10 ma reactivation of the Southern Yin shan, North China, revealed by low-temperature Thermochronology, " *Tectonophysics*, vol. 823, January, p. 229189, 2022.

[33] Z. Y. Fu, X. Q. Yuan, and G. C. Geng, "The tertiary of the Hetao basin and its Biotas," *Journal of Stratigraphy*, vol. 18, no. 1, pp. 24–29, 1994.

[34] Q. Q. Xu, J. Q. Ji, W. T. Zhao, and X. J. Yu, "Uplift-Exhumation history of Daqing mountain, inner Mongolia, since late Mesozoic," *Acta Scientiarum Naturalium Universitatis Pekinensis*, vol. 53, pp. 57–65, 2017.

[35] L. X. Feng, B. F. Han, Z. Z. Wang, et al., "Differential uplift-Denudation of the basement in the Daqingshan mountains, inner Mongolia, since the late Mesozoic: Constraints from the Apatite fission track Thermochronology," *Acta Geologica Sinica*, vol. 95, no. 6, pp. 1727–1742, 2021.

[36] S. P. Cheng, Q. D. Deng, G. Z. Yang, and D. W. Ren, "On the Cenozoic Denudation and uplift of the Daqingshan mountains, Nei Monggol," *Seismolgy and Geology*, vol. 22, pp. 27–36, 2000.

[37] Bureau of Geology and Mineral Resources of Nei Mongol Autonomous Region, "Regional geology of Nei Mongol (inner Mongolia) autonomous region," in *Geological Memoirs, Series*. Vol. 25, Geological Publishing House, Beijing, 1991.

[38] B. D. Ritts, A. K. Berry, C. L. Johnson, B. J. Darby, and G. A. Davis, "Early Cretaceous Supradetachment basins in the Hohhot metamorphic core complex, inner Mongolia, China," *Basin Research*, vol. 22, no. 1, pp. 45–60, 2010. http://blackwell-synergy.com/doi/abs/10.1111/bre.2010.22.issue-1.

[39] Y. Wan, P. Peng, S. Liu, et al., "Late Paleoproterozoic Tectono-thermal event in the Northwestern North China Craton: Evidence from U-PB dating and O-HF isotopic compositions of Zircons from Metasedimentary rocks north of Hohhot city, inner Mongolia, northern China," *Journal of Asian Earth Sciences*, vol. 167, November, pp. 152–164, 2018.

[40] C. Zhang, B. F. Han, S. W. Liu, J. Q. Ji, L. Zhao, and L. Zhang, "Shrimp U-PB dating of Biotite Granites in Daqingshan, inner Mongolia， and its significance," *Acta Petrologica Sinica*, vol. 25, no. 3, pp. 561–567, 2009.

[41] L. Guo, T. Wang, J. J. Zhang, J. Liu, G. W. Qi, and J. B. Li, "Evolution and time of formation of the Hohhot metamorphic core complex, North China. New structural and Geochronological evidence," *International Geology Review*, vol. 54, no. 11, pp. 1309–1331, 2012.

[42] Q. P. Meng, Y. K. He, W. Zhang, et al., "Time constraints on the inversion of the Tectonic regime in the northern margin of the North China Craton: Evidence from the Daqingshan Granites," *Journal of Asian Earth Sciences*, vol. 79, January, pp. 246–259, 2014.

[43] Y. Zheng, G. A. Davis, C. Wang, B. J. Darby, and Y. Hua, "Major thrust sheet in the Daqing shan mountains, inner Mongolia, China," *Science in China Series D*, vol. 41, no. 5, pp. 553–560, 1998.

[44] G. A. Davis, W. Cong, Z. Yadong, Z. Jinjiang, Z. Changhou, and G. E. Gehrels, "The enigmatic Yinshan fold-and-thrust belt of northern China: new views on its Intraplate Contractional styles," *Geology*, vol. 26, no. 1, p. 43, 1998.

[45] G. A. Davis, B. J. Darby, Z. Yadong, and T. L. Spell, "Geometric and temporal evolution of an Extensional detachment fault, Hohhot metamorphic core complex, inner Mongolia, China," *Geology*, vol. 30, no. 11, p. 1003, 2002.

[46] J. J. Zhang, G. W. Qi, L. Guo, and J. Liu, "$^{40}Ar/^{39}Ar$ dating of the Mesozoic thrusting in Daqingshan thrust-Nappe system, inner Mongolia, China," *Acta Petrologica Sinica*, vol. 25, pp. 609–620, 2009.

[47] G. A. Davis and B. J. Darby, "Early Cretaceous Overprinting of the Mesozoic Daqing shan fold-and-thrust belt by the Hohhot metamorphic core complex, inner Mongolia, China," *Geoscience Frontiers*, vol. 1, no. 1, pp. 1–20, 2010.

[48] J. Liu, J. J. Zhang, L. Guo, and G. W. Qi, "$^{40}Ar/^{39}Ar$ dating of the detachment fault of the Hohhot metamorphic core complex, inner Mongolia, China," *Acta Petrologica Sinica*, vol. 30, pp. 1899–1908, 2014.

[49] W. Gong, J. Hu, H. Chen, Z. Li, H. Qu, and Y. Yang, "Late Mesozoic Tectonic evolution and Kinematic mechanisms in the Daqing shan at the northern margin of the North China Craton," *Journal of Asian Earth Sciences*, vol. 114, December, pp. 103–114, 2015.

[50] S. Y. Zhu, "Nappe Tectonics in Sertengshan-Daqingshan, inner Mongolia," *Geology of Inner Mongolia*, vol. 1, pp. 41–47, 1997.

[51] Changqing Oilfield Petroleum Geological Records Writing Group, *Petroleum Geology of China Vol 12: Changqing Oil Field*, Petroleum Industry Press, Beijing, 1992.

[52] Y. K. Ran, P. Z. Zhang, and L. C. Chen, "Research on the COMP lateness of Paleoseismic activity history since late Quaternary along the Daqingshan Piedmont fault in Hetao depression zone, North China," *Earth Science Frontiers (China University of Geosciences, Beijing)*, vol. 10, no. S1, pp. 207–216, 2003.

[53] L. Hu and H. L. Song, "Ages of activities of the Southern "inner Mongolian axis" marginal fault belt and an analysis of its structure," *Geology in China*, vol. 29, no. 4, pp. 369–373, 2002.

[54] P. Vermeesch, "Helioplot, and the treatment of Overdispersed (U-th-Sm)/He data," *Chemical Geology*, vol. 271, nos. 3–4, pp. 108–111, 2010.

[55] C. Gautheron, L. Tassan-Got, J. Barbarand, and M. Pagel, "Effect of alpha-damage Annealing on Apatite (U–Th)/He Thermochronology," *Chemical Geology*, vol. 266, nos. 3–4, pp. 157–170, 2009.

[56] L. Wu, G. H. Shi, M. Danišík, Z. Y. Zhang, Y. Wang, and F. Wang, "MK-1 Apatite: A new potential reference material for (U-Th)/He dating," *Geostandards and Geoanalytical Research*, vol. 43, no. 2, pp. 301–315, 2019. .

[57] L. Wu, F. Wang, Z. Y. Zhang, et al., "Reappraisal of the applicability of MK-1 Apatite as a reference standard for (U-Th)/He Geochronology," *Chemical Geology*, vol. 575, August, p. 120255, 2021.

[58] L. Wu, P. Monié, F. Wang, et al., "Cenozoic Exhumation history of Sulu Terrane: Implications from (U–Th)/He Thermochrology," *Tectonophysics*, vols. 672–673, March, pp. 1–15, 2016.

[59] R. A. Ketcham, "Forward and inverse modeling of low-temperature thermo-chronometry data," *Reviews in Mineralogy and Geochemistry*, vol. 58, no. 1, pp. 275–314, 2005.

[60] R. M. Flowers, R. A. Ketcham, D. L. Shuster, and K. A. Farley, "Apatite (U-Th)/He Thermochronometry using a radiation damage accumulation and Annealing model," *Geochimica et Cosmochimica Acta*, vol. 73, no. 8, pp. 2347–2365, 2009.

[61] R. W. Brown, R. Beucher, S. Roper, C. Persano, F. Stuart, and P. Fitzgerald, "Natural age dispersion arising from the analysis of broken crystals. part I: theoretical basis and implications for the Apatite (U–Th)/He Thermochronometer," *Geochimica et Cosmochimica Acta*, vol. 122, December, pp. 478–497, 2013.

[62] K. A. Farley, "(U-Th)/He dating: Techniques, calibrations, and applications," *Reviews in Mineralogy and Geochemistry*, vol. 18, pp. 819–844, 2002.

[63] P. W. Reiners and K. A. Farley, "Influence of crystal size on Apatite (U–Th)/He Thermochronology: An example from the Bighorn mountains, Wyoming," *Earth and Planetary Science Letters*, vol. 188, nos. 3–4, pp. 413–420, 2001.

[64] D. L. Shuster, R. M. Flowers, and K. A. Farley, "The influence of natural radiation damage on helium diffusion Kinetics in Apatite," *Earth and Planetary Science Letters*, vol. 249, nos. 3–4, pp. 148–161, 2006.

[65] K. A. Farley, D. L. Shuster, and R. A. Ketcham, "U and th Zonation in Apatite observed by laser ablation ICPMS, and implications for the (U–Th)/He system," *Geochimica et Cosmochimica Acta*, vol. 75, no. 16, pp. 4515–4530, 2011.

[66] R. M. Flowers and S. A. Kelley, "Interpreting data dispersion and "inverted" dates in Apatite (U–Th)/He and fission-track Datasets: An example from the US Midcontinent," *Geochimica et Cosmochimica Acta*, vol. 75, no. 18, pp. 5169–5186, 2011.

[67] T. A. Ehlers and K. A. Farley, "Apatite (U-Th)/He Thermochronometry: Methods and applications to problems in Tectonic and surface processes," *Earth and Planetary Science Letters*, vol. 206, nos. 1–2, pp. 1–14, 2003.

[68] C. Y. Liu, H. G. Zhao, X. J. Gui, Y. P. Yue, J. F. Zhao, and J. Q. Wang, "Space-time coordinate of the evolution and reformation and mineralization response in Ordos Basin," *Acta Geologica Sinica*, vol. 80, no. 5, pp. 617–638, 2006.

[69] C. Clinkscales, P. Kapp, and H. Wang, "Exhumation history of the North-central Shanxi rift, North China, revealed by low-temperature Thermochronology, " *Earth and Planetary Science Letters*, vol. 536, April, p. 116146, 2020. https://doi.org/10.1016/j.epsl.2020.116146.

[70] W. Zhang, F. Wang, L. Wu, et al., "Reactivated margin of the Western North China Craton in the late Cretaceous: Constraints from Zircon (U-Th)/He Thermochronology of Taibai mountain," *Tectonics*, vol. 41, no. 2, p. 2021TC007058, 2022.

[71] Z. H. Wu and Z. H. Wu, "Low-temperature Thermochronological analysis of the uplift history of the Yanshan mountain and its neighboring area," *Acta Geologica Sinica*, vol. 77, no. 3, pp. 399–406, 2003.

[72] L. Wu, F. Wang, W. Lin, et al., "Rapid cooling of the Yanshan belt, northern China: Constraints from $^{40}Ar/^{39}Ar$ Thermochronology and implications for Cratonic Lithospheric thinning," *Journal of Asian Earth Sciences*, vol. 90, August, pp. 107–126, 2014.

[73] J. Chang, N. S. Qiu, S. Liu, C. E. Cai, Q. C. Xu, and N. Liu, "Post-Triassic multiple Exhumation of the Taihang mountains revealed via low-T Thermochronology: Implications for the paleo-Geomorphologic reconstruction of the North China Craton," *Gondwana Research*, vol. 68, April, pp. 34–49, 2019.

[74] L. Wu, F. Wang, J. Yang, et al., "Meso-Cenozoic uplift of the Taihang mountains, North China: Evidence from Zircon and Apatite Thermochronology," *Geological Magazine*, vol. 157, no. 7, pp. 1097–1111, 2020.

[75] H. S. Sun, H. Li, L. Liu, Q. M. Chen, H. Yang, and P. Wu, "Exhumation history of the Jiaodong and its adjacent areas since the late Cretaceous: Constraints from low temperature Thermochronology," *Science China Earth Sciences*, vol. 60, no. 3, pp. 531–545, 2017.

[76] L. Wu, P. Monié, F. Wang, W. Lin, W. B. Ji, and L. K. Yang, "Multi-phase cooling of early Cretaceous Granites on the Jiaodong peninsula, East China: Evidence from $^{40}Ar/^{39}Ar$ and (U-Th)/He Thermochronology," *Journal of Asian Earth Sciences*, vol. 160, July, pp. 334–347, 2018.

[77] X. M. Li, G. L. Gong, X. Y. Yang, and Q. S. Zeng, "Late Cretaceous–Cenozoic Exhumation of the Yanji area, NE China: Constraints from fission track Thermochronology," *Island Arc*, vol. 19, no. 1, pp. 120–133, 2010. http://blackwell-synergy.com/doi/abs/10.1111/iar.2010.19.issue-1.

[78] C. Wu, *Landform Environment and Its Formation in North China*, Science Press, Beijing, 2008.

[79] J. Xu, Z. W. Gao, J. B. Sun, and C. Q. Song, "A preliminary study of the coupling relationship between basin and mountain in Extensional environments—a case study of the Bohai Bay basin and Taihang mountain," *Acta Geologica Sinica*, vol. 75, no. 2, pp. 165–174, 2001.

[80] Y. Ju, K. Yu, G. Wang, et al., "Coupling response of the Meso-Cenozoic differential evolution of the North China Craton to Lithospheric structural transformation," *Earth-Science Reviews*, vol. 223, December, p. 103859, 2021.

[81] Y. Q. Zhang, S. W. Dong, and W. Shi, "Cretaceous deformation history of the middle tan-LU fault zone in Shandong province, Eastern China," *Tectonophysics*, vol. 363, nos. 3–4, pp. 243–258, 2003.

[82] S. Dong, Y. Zhang, H. Li, et al., "The Yanshan Orogeny and late Mesozoic multi-plate convergence in East Asia—commemorating 90th years of the "Yanshan Orogeny", *Science China Earth Sciences*, vol. 61, no. 12, pp. 1888–1909, 2018.

[83] Y. T. Yang, "An unrecognized major collision of the Okhotomorsk block with East Asia during the late Cretaceous, constraints on the plate reorganization of the Northwest Pacific," *Earth-Science Reviews*, vol. 126, November, pp. 96–115, 2013.

[84] W. Zhang, F. Wang, L. Wu, et al., "Mountain growth under the combined effects of Paleostress and Paleoclimate: Implications from Apatite (U-Th)/He Thermochronology of Taibai mountain, central China," *Lithosphere*, vol. 2022, no. 1, 2022.

[85] J. F. Zhao, Y. C. Liu, N. Mountney, J. J. Lu, Y. Yang, and R. Xue, "Timing of uplift and evolution of the Lvliang mountains, North China Craton," *Science China (Earth Sciences*), vol. 45, pp. 1427–1438, 2016.

[86] Z. G. Huang, Q. R. Zheng, E. H. Sun, and D. D. Wang, "Fission track evidence of Tectonic evolution of the Paleoproterozoic Granitic Pluton in the North-central part of Lvliang mountain," *Acta Geologica Sinica*, vol. 92, pp. 1216–1227, 2018.

[87] J. X. Li, C. X. Liu, L. P. Yue, and J. Q. Wang, "Apatite fission track evidence for the Cenozoic uplift of the Lvliang Muntains and a discussion on the uplift mechanism," *Geology in China*, vol. 42, pp. 960–972, 2015.

[88] J. Liang, H. Wang, Y. Bai, X. Ji, and X. Duo, "Cenozoic Tectonic evolution of the Bohai Bay basin and its coupling relationship with Pacific plate Subduction," *Journal of Asian Earth Sciences*, vol. 127, September, pp. 257–266, 2016.

[89] Y. B. Zhu, S. F. Liu, B. Zhang, M. Gurnis, and P. F. Ma, "Reconstruction of the Cenozoic deformation of the Bohai Bay Basin, North China," *Basin Research*, vol. 33, no. 1, pp. 364–381, 2021. https://onlinelibrary.wiley.com/toc/13652117/33/1.

[90] G. Z. Wang, S. Z. Li, Y. H. Suo, et al., "Deep-shallow coupling response of the Cenozoic Bohai Bay Basin to plate interactions around the Eurasian plate," *Gondwana Research*, vol. 102, February, pp. 180–199, 2022.

[91] S. Hu, A. Raza, K. Min, et al., "Late Mesozoic and Cenozoic Thermotectonic evolution along a Transect from the North China Craton through the Qinling Orogen into the Yangtze Craton, central China," *Tectonics*, vol. 25, no. 6, p. n, 2006.

[92] L. Li and D. L. Zhong, "Fission track evidence of Cenozoic Uplifting events of Taishan mountain, China," *Acta Petrologica Sinica*, vol. 22, no. 2, pp. 457–464, 2006.

[93] L. S. Shu, B. Wang, L. S. Wang, and G. Y. He, "Analysis of northern Jiangsu prototype Basin from late Cretaceous to Neogene," *Geological Journal of China Universities*, vol. 11, no. 4, pp. 534–543, 2006.

[94] G. Chen, Z. Y. Zhao, P. L. Li, et al., "Fission track evidence for the Tectonic–thermal history of the Hefei Basin," *Chinese Journal of Geophysics*, vol. 48, no. 6, pp. 1433–1442, 2005.

[95] X. Cao, S. Li, L. Xu, et al., "Mesozoic to the Cenozoic evolution and mechanism of Tectonic Geomorphology in the central North China block: constrains by Apatite fission track Thermochronology," *Journal of Asian Earth Sciences*, vol. 114, December, pp. 41–53, 2015.

[96] X. Huang, Y. N. Wang, J. Zhang, F. Z. Wu, and Y. L. Yang, "Low-temperature Thermochronological insights into the Mesozoic–Cenozoic Exhumation history of the Taihang–Lvliangshan region: A review," *Geological Journal*, vol. 57, no. 4, pp. 1511–1529, 2022. https://onlinelibrary.wiley.com/toc/10991034/57/4.

[97] S. B. Li, Y. J. Wang, Y. Z. Zhang, L. M. Zhang, H. Liang, and W. Qiu, "Meso-Cenozoic Uplifting of South Taihang mountains: Constraints from Apatite fission track data," *Geotectonica et Metallogenia*, vol. 39, pp. 460–469, 2015.

[98] M. Seton, R. D. Müller, S. Zahirovic, et al., "Global Continental and ocean Basin Reconstructions since 200Ma," *Earth-Science Reviews*, vol. 113, nos. 3–4, pp. 212–270, 2012.

[99] J. Wu, Y. A. Lin, N. Flament, J. T. J. Wu, and Y. D. Liu, "Northwest Pacific-Izanagi plate Tectonics since Cretaceous times from Western Pacific Mantle structure," *Earth and Planetary Science Letters*, vol. 583, April, p. 117445, 2022.

[100] M. Jolivet, M. Brunel, D. Seward, et al., "Mesozoic and Cenozoic Tectonics of the northern edge of the Tibetan plateau: Fission-track constraints," *Tectonophysics*, vol. 343, nos. 1–2, pp. 111–134, 2001.

[101] A. Yin, P. E. Rumelhart, R. Butler, et al., "Tectonic history of the Altyn Tagh fault system in northern Tibet inferred from Cenozoic sedimentation," *Geological Society of America Bulletin*, vol. 114, no. 10, pp. 1257–1295, 2002.

[102] M. K. Clark, K. A. Farley, D. W. Zheng, Z. Wang, and A. R. Duvall, "Early Cenozoic Faulting of the northern Tibetan plateau margin from Apatite (U-Th)/He ages," *Earth and Planetary Science Letters*, vol. 296, nos. 1–2, pp. 78–88, 2010.

[103] X. H. Chen, W. M. Michael, L. Li, et al., "Thermochronological evidence for multi-phase Uplifting of the east Kunlun mountains, northern Tibetan plateau," *Geological Bulletin of China*, vol. 30, no. 11, pp. 1647–1660, 2011.

[104] Y. D. Wang, J. J. Zheng, Y. W. Zheng, X. Liu, and G. Sun, "Paleocene-early Eocene uplift of the Altyn Tagh mountain: Evidence from Detrital Zircon fission track analysis and seismic sections in the Northwestern Qaidam Basin," *Journal of Geophysical Research*, vol. 120, no. 12, pp. 8534–8550, 2015. https://onlinelibrary.wiley.com/toc/21699356/120/12.

[105] C. Wu, A. V. Zuza, J. Li, et al., "Late Mesozoic–Cenozoic cooling history of the Northeastern Tibetan plateau and its foreland derived from low-temperature Thermochronology," *GSA Bulletin*, vol. 133, nos. 11–12, pp. 2393–2417, 2021.

[106] M. K. Clark, K. A. Farley, D. W. Zheng, Z. C. Wang, and A. R. Duvall, "Early Cenozoic Faulting of the northern Tibetan plateau margin from Apatite (U–Th)/He ages," *Earth and Planetary Science Letters*, vol. 296, nos. 1–2, pp. 78–88, 2010.

[107] M. Liu, X. J. Cui, and F. T. Liu, "Cenozoic Rifting and Volcanism in Eastern China: A Mantle dynamic link to the Indo–Asian collision," *Tectonophysics*, vol. 393, nos. 1–4, pp. 29–42, 2004.